ACS APPLIED MATERIALS & INTERFACES

Research Article

Cite This: ACS Appl. Mater. Interfaces 2020, 12, 1799−1805

www.acsami.org

An Optical Microfiber Biosensor for CEACAM5 Detection in Serum: Sensitization by a Nanosphere Interface

Aoxiang Xiao, Yunyun Huang,* Jiaying Zheng, Pengwei Chen, and Bai-Ou Guan

Guangdong Provincial Key Laboratory of Optical Fiber Sensing and Communications, Institute of Photonics Technology, Jinan University, Guangzhou 511486, China

Supporting Information

ABSTRACT: The detection of carcinoembryonic antigen (CEA)-related cell adhesion molecules 5 (CEACAM5) is significant in cancer prewarning. Early diagnosis can effectively alleviate the danger of cancer. Point-of-care testing (POCT) has become a competitive technology for early detection. Fiber optic biosensors have great potential as POCT tools. However, their limits of detection (LODs) are not sufficient to afford ultralow concentration detection at the early stage. Herein, this work presents an optical microfiber sensor functionalized by a polystyrene@gold nanosphere (PS@Au nanosphere) interface for a synergistic sensitization effect to detect the ultralow CEACAM5 concentrations in serum at the early stage. The sensor's LOD achieves 3.54×10^{-17} M in pure solution and 5.27×10^{-16} M in serum, with the sensitization effect coupled with surface area enlargement and electromagnetic enhancement of interface. This LOD is about 6 orders of magnitude lower than that of current methods. It can be employed to detect the biomarkers at ultralow concentrations present in serum in the early stages of cancer. As the interfacial synergistic sensitization strategy is suitable for refractive index (RI)-based optical transducers, this work provides new opportunities to employ fiber optic biosensors as effective POCT tools.

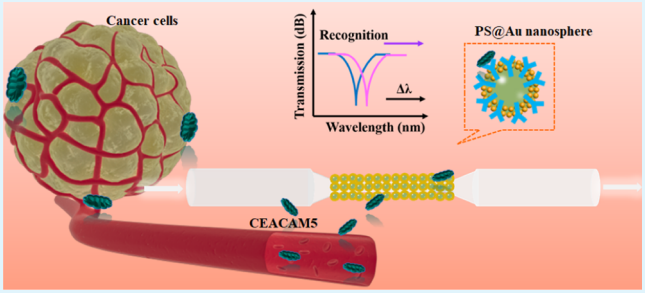

KEYWORDS: *early detection, optical microfiber, biosensor, interfacial sensitization, in serum*

INTRODUCTION

Human health has long been threatened by cancers. Early diagnosis can significantly alleviate the harm. Protein cancer biomarkers, playing important roles in the prognosis, diagnosis, and therapy of cancers, can be found in serum, tissue, and body fluids. Their concentration detection is considered an important basis for cancer diagnosis.[1] The carcinoembryonic antigen (CEA)-related cell adhesion molecules 5 (CEACAM5), belonging to the CEACAM family,[2] is overexpressed in many cancers,[3−6] for example, most gastrointestinal, colorectal, and pancreatic cancers. Functioning as a chemoattractant and as an adhesion molecule, CEACAM5 has been reported to promote metastatic potential in some experimental tumors.[7] Its detection is significant in cancer prewarning. Currently, immunoassays and related techniques[2,8,9] have been considered as major analytical methods for CEACAM5 detection. These works detected CEACAM5 in tissues, cancer cells, and pure solution, respectively. The emerging point-of-care testing (POCT), in vitro diagnostic tests that can provide the result without involving laboratory staff and facilities,[10] offering detecting methods with the advantages of expanding diagnostic accessibility, reducing costs, and rapid analysis time,[11] has become a competitive technology for early detection,[12] which may be employed in CEACAM5 measurement. The POCT requires the ability to detect CEACAM5 in blood or serum. However, the concentration of this biomarker in blood or serum is much lower than that in tissues or cancer cells at the early stage. Therefore, the POCT sensors for CEACAM5 should be of high sensitivity. Fiber optic biosensors, with their low cost, flexibility, and millimeter-scale length, have the potential for use as POCT devices.[12] However, their relatively low sensitivity at picomolar concentrations[13] strongly hinders their use in the early-stage detection of CEACAM5.

In recent years, researchers have focused on enhancing fiber sensitivity through exploring the sensing mechanism from different perspectives.[14−17] Based on this, optical fibers with various structures, including fiber coupler,[18] fiber Fabry−Perot cavity,[19] and whispering gallery modes,[15] have been developed. The structures of these fibers are relatively complex. Optical microfiber, which is easy to fabricate, is especially suitable for POCT after surface functionalization. Since the refractive index (RI)-based microfiber biosensor captures fiber surface RI change caused by molecular binding interactions via its evanescent field,[20] it is efficient to improve the sensitivity by increasing the assembly surface area and reducing the difficulty of antibody immobilizing. Some efforts have been made to increase the surface area of microfiber, and this approach has

Received: September 17, 2019
Accepted: December 12, 2019
Published: December 12, 2019

DOI: 10.1021/acsami.9b16702
ACS Appl. Mater. Interfaces 2020, 12, 1799−1805

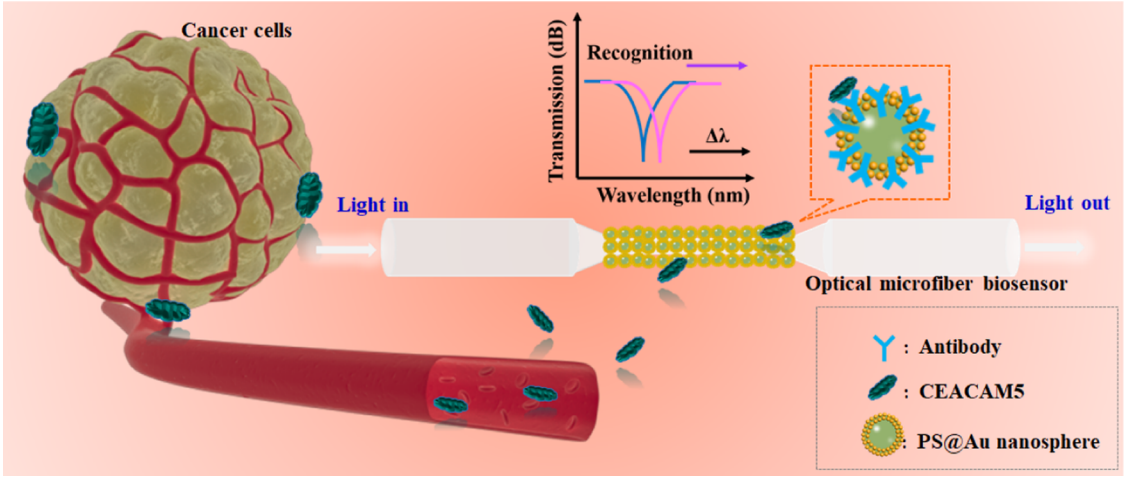

Figure 1. Scheme of the PS@Au nanosphere interface-functionalized optical microfiber for the detection of the cancer cell protein biomarker CEACAM5.

been shown to improve the sensitivity to some extent.[21,22] As the evanescent field is also an important factor in determining microfiber's sensitivity, the synergy of increasing the assembly surface area and enhancing the evanescent field might help to have an exciting effect in the sensitivity improvement. Herein, we demonstrate an optical microfiber sensor functionalized by a polystyrene@gold nanosphere (PS@Au nanosphere) interface for a synergistic sensitization effect to detect the ultralow CEACAM5 concentrations at the early stage. The nanospheres on the interface are employed to increase the assembly area and reduce the difficulty of antibody immobilizing to increase the amount of CEACAM5 probes and to stabilize them on the fiber surface,[21] while the gold nanoshells on the PS nanosphere surface enhance the evanescent field through electromagnetic enhancement.[23] Based on the interfacial synergistic sensitization of the PS@Au nanosphere interface, the optical microfiber sensor presents a linear response and an ultrahigh sensitivity of 0.86 nm/lg M within 5 orders of concentration (10^{-16}–10^{-11} M). The limit of detection (LOD) of the sensor for the concentration of CEACAM5 molecules is as low as 3.54×10^{-17} M in pure solution, 6 orders of magnitude lower than that of current methods (10^{-10} M).[8] The sensor realizes the CEACAM5 sensing in serum in the early stage with an LOD of 5.27×10^{-16} M, which might be the lowest LOD of this biomarker realized by sensors in the serum to our knowledge. The interfacial synergistic sensitization strategy implemented by enlarging the assembly surface area and reducing the difficulty of antibody immobilizing, as well as enhancing the electromagnetic field shows a universal method for optical fiber sensitization. This highly sensitive, miniaturized device provides an effective tool for POCT.

RESULTS AND DISCUSSION

As an adhesion molecule, CEACAM5 plays important roles in cancer metastasis and adhesion. In the early stage or prognosis of cancers, the CEACAM5 concentration in serum is significantly lower than that in cancer cells or tissues. But as a POCT device, it is obviously more convenient to detect this biomarker in serum than in cancer cells or tissues. As shown in Figure 1, when the CEACAM5 molecules peel off the surface of cancer cells and enter the blood, the sensor was used to detect their concentration in serum. The optical microfiber sensor was functionalized by the PS@Au nanosphere interface. The PS@Au nanospheres were modified with a specific CEACAM5 antibody that was used to capture CEACAM5 proteins in solutions. In this work, we used the anti-CEACAM5 antibody for binding CEACAM5 with high affinity and selectively. The PS@Au nanospheres coated with the CEACAM5 antibody were constructed on the surface of silica microfiber, forming a single-layer nanointerface. After the binding of CEACAM5 molecules on the microfiber surface, the transmission of the optical microfiber sensor was found to redshift with increasing surface RI.

The PS@Au nanospheres employed in this work were prepared as shown in Figure 2. The gold nanoparticles with carboxyl groups on the surface bonded on the surface of amino group-modified PS nanospheres through an activation with EDC and NHS[24] (Figure 2a). According to the scanning electron microscopy (SEM) images in Figure 2b,c, core–shell nanospheres with diameters of ∼200 nm were obtained. Energy-dispersive spectroscopy (EDS) analysis was carried out on several typical particles to investigate the composition of these nanospheres, and it was found that each nanoparticle was composed of the elements C and Au (Figure 2d). It is apparent in the EDS mapping that the C was mainly distributed in the interior of the nanospheres, while the Au was distributed on the coating as a ring, indicating the core–shell structure of the obtained nanospheres. Figure 2e shows the UV–vis absorption spectra of Au nanoparticles before and after the core–shell nanosphere functionalization. It indicates that the Au particles behaved as discrete but coupled particles and not as a thin, continuous metal ring.[25] These results confirm the formation of PS@Au nanospheres.[26]

Figure 3a presents the interface functionalization process of the optical microfiber sensor. The PS@Au nanosphere surface was modified by glutaraldehyde solution, and the CEACAM5 antibody was then injected into the nanosphere dispersion. The acetal bridges derived by glutaraldehyde combined the antibody on the PS surface.[27] The PS surface rich in π electrons made it easier for the antibody to immobilize on it than directly on the silica microfiber surface.[28] It allowed the antibody to bind more tightly and firmly on the PS nanosphere than it could on a silica surface with the same surface area. Then, the optical microfiber was immersed in a piranha solution to produce hydroxyl groups, modifying the fiber surface with negative charges.[29] Subsequently, the amino

DOI: 10.1021/acsami.9b16702
ACS Appl. Mater. Interfaces 2020, 12, 1799–1805

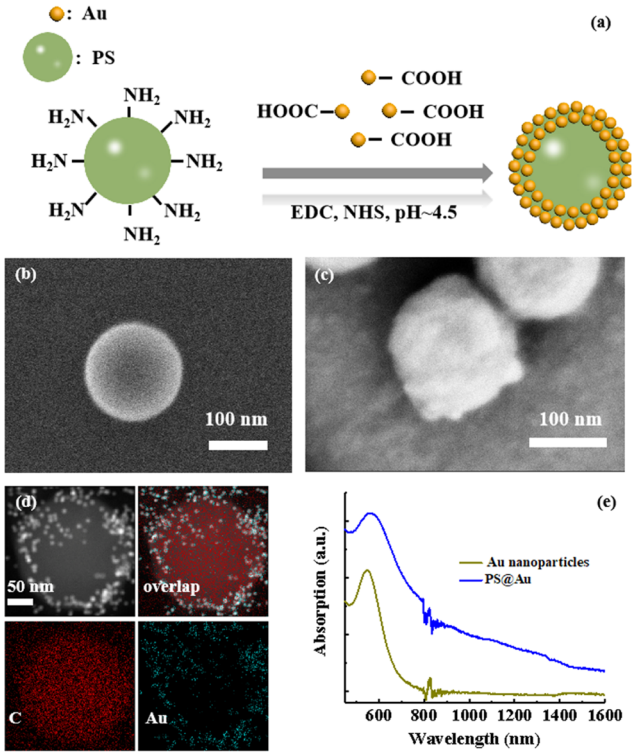

Figure 2. Preparation of PS@Au nanospheres. (a) Scheme of the preparation process of PS@Au nanospheres. (b) SEM image of the PS nanosphere, (c) SEM image of the PS@Au nanosphere, (d) EDS mapping of an as-prepared PS@Au nanosphere, (e) UV−vis absorption spectra of Au nanoparticles and PS@Au nanospheres (The Au nanoparticles and PS@Au nanospheres were in the solid state.).

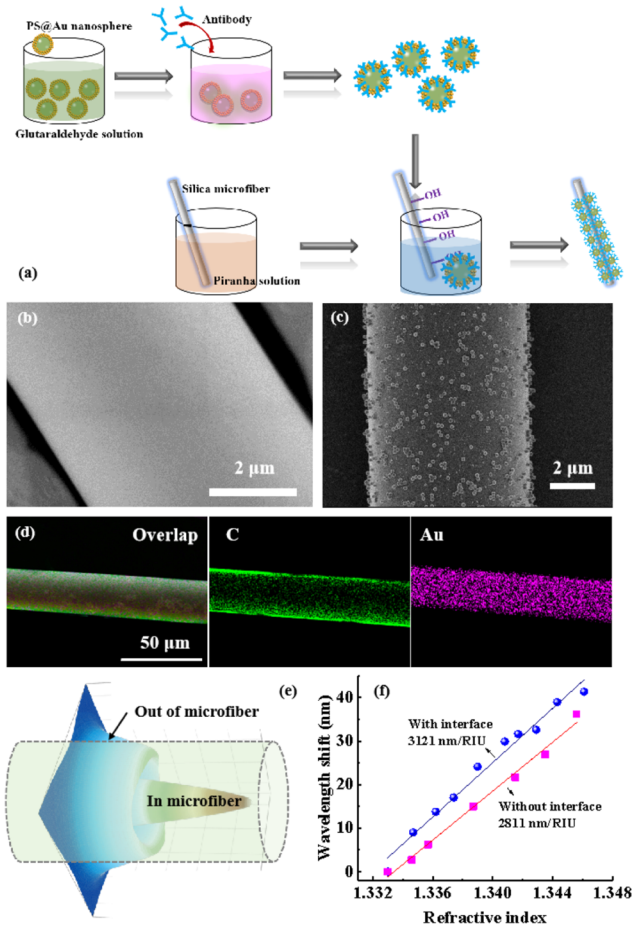

Figure 3. Preparation of the PS@Au nanosphere interface-functionalized optical microfiber sensor. (a) Scheme of the preparation process of a PS@Au nanosphere interface-functionalized optical microfiber sensor. SEM images of microfiber before (b) and after (c) PS@Au nanosphere interface functionalization. (d) EDS mapping of the microfiber surface after PS@Au nanosphere functionalization. (The diameter of the silica microfiber used in the EDS test was a little larger than that of the as-prepared sensor because of the EDS resolution.) (e) Scheme diagram of the HE_{12} mode in the silica microfiber at 1550 nm wavelength. (f) RI sensitivity of silica microfiber and microfiber with the PS@Au nanosphere interface.

groups of antibodies on the PS@Au nanospheres and the hydroxyl groups on the microfiber attracted each other by electrostatic attraction[23] to achieve nanosphere interface functionalization on the microfiber. The SEM images of the microfiber surface before and after interface functionalization in Figure 3b,c and the EDS mapping of the microfiber after interface functionalization in Figure 3d demonstrate the successful construction of a single-layer interface.

The RI-based optical microfiber biosensor detected the fiber surface RI change via its evanescent field.[20] The mode coupling in the microfiber was produced by the interferometer's geometry.[30] The fundamental core mode of uptapered fiber excited the fundamental core mode (HE_{11}) and higher-order modes (HE_{12}) when it entered the downtapered region. The HE_{12} presented a higher change rate according to the RI change due to its larger fractional power of the optical field guided outside the microfiber as the evanescent field.[31] For a 7.5 μm-diameter microfiber, approximately 20% of the HE_{12} mode evanesced as the evanescent field (Figure 3e), which appeared on the microfiber surface and interacted with the surroundings.[32] Figure 3f shows the bulk RI sensitivities of the silica microfiber and the microfiber with the PS@Au nanosphere interface. This result demonstrates that the microfiber with the interface showed a nonobvious higher bulk RI sensitivity than that of silica microfiber without an interface. The sensitivity to the whole solution was not significantly enhanced. This indicates that the interfacial sensitization effect focuses on the microfiber surface, but does not uniformly enhance the whole evanescent field. This makes it suitable as a biosensor that captures target molecules on its surface, and more likely to avoid the interference from a distant solution of the microfiber surface. After the interface functionalization, the optical microfiber sensor was ready for CEACAM5 detection.

The CEACAM5 detection ability of the as-prepared sensor was evaluated, as shown in Figure 4, along with a control experiment (the microfiber sensor without an interface). The wavelength stability of the as-prepared sensor in phosphate-buffered saline (PBS) solution is shown in Figure S1. As shown in Figure 4a, the sensor displayed spectral modulation when it was exposed to CEACAM5 solutions (concentrations: 0−10^{-10} M). With an increase in CEACAM5 concentrations from 10^{-16} to 10^{-11} M, redshifts of spectrum with a sensitivity of 0.86 nm/lg M (linearity: 99.4%) were observed, as shown in Figure 4b. It is worth noting that the LOD[33] was 3.54×10^{-17} M, 6 orders of magnitude lower than the recent CEACAM5 measurement methods (10^{-10} M).[8] As a control experiment, the microfiber sensor without any interface exhibited poorer detecting performance (Figure 4b). The as-prepared sensor

DOI: 10.1021/acsami.9b16702
ACS Appl. Mater. Interfaces 2020, 12, 1799−1805

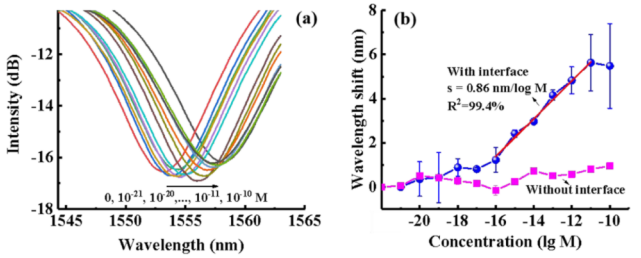

Figure 4. Transmission spectra of the (a) microfiber sensor with the PS@Au nanointerface responding to various concentrations of CEACAM5 solution and (b) corresponding wavelength shifts of the microfiber sensor with a PS@Au nanointerface and control sensor (silica microfiber without an interface).

showed an LOD about 5 orders of magnitude lower than the control sensor's output. The control experiments in Figure S2 also presented the sensing abilities of microfiber sensors with different but similar interfaces: the PS@Au interface without antibodies, the PS interface with antibodies but without Au NPs, the Au NPs interface directly functionalized on the microfiber without antibodies and PS nanospheres, and the mixture interface without good PS/Au contact (the PS nanospheres with antibodies were functionalized on microfiber first and then the Au NPs were added to the microfiber surface). All of these control microfiber sensors showed poorer sensing performance than that of the as-prepared sensor. This indicated that the PS@Au nanosphere interface played an important role in improving the sensor's sensitivity.

Comparing the other control interfaces and the PS@Au–antibody interface of the as-prepared sensor, it can be found that the antibody played a role of specific recognition and binding the target molecules in the sensing (Figure S3 shows that the sensors without the antibody presented poor selectivity.) As the binding ability to targets was weakened, the sensitivities of the control sensors were significantly reduced (Figure S2a,c). This was consistent with the bulk RI sensitivity obtained in Figure 3f, demonstrating that the as-prepared interface enhanced the surface RI sensitivity of the sensor rather than the bulk RI sensitivity. The PS nanosphere interface without Au nanoparticles (with antibody) could only increase the quantity and stability of antibodies assembling on the interface but could not enhance the electromagnetic field on the surface. Thus, the obtained sensitivity was also poorer than the as-prepared sensor (Figure S2b). The interface containing only Au NPs without the shaping effect of PS nanosphere and the interface with poor interacting between PS nanospheres and Au NPs presented much poorer sensitivities (Figure S2c,d). This might due to the weak interaction between Au NPs and the microfiber surface, which might result in some Au NPs falling off during the detection. In view of the surface RI sensitivity enhancement, the enhancement effect of the nanosphere interface has been explored in two ways: increasing the quantity and stability of antibodies assembling on the interface and enhancing the electromagnetic field on the surface.

For the monolayer nanospheres, if they were packed densely and uniformly, 44.08 nanospheres/μm^2 could be assembled on the microfiber surface. As the number of nanospheres on the microfiber surface was at most 2/3 according to the SEM image in Figure 3c, the number of nanospheres per μm^2 was assumed to be 25 here based on a conservative estimation. Thus, the nanosphere interface provided 2.3 μm^2 per μm^2 microfiber surface. That is, the nanosphere interface enlarged the antibody assembly surface 2.3 times. The enlargement of the assembly surface area increased the amount of antibody on the microfiber surface. This augmentation also enhanced the capture ability versus the CEACAM5 targets, which enhanced the sensitivity of the sensor.[21] Additionally, it was easier to immobilize the antibodies on the PS nanosphere surface than on the silica fiber surface.[29] (The delocalized π-electrons in the aromatic ring of PS surface[34] interacted with the electrons of aldehyde groups of glutaraldehyde, making the glutaraldehyde distribute on its surface evenly and closely. This led to an easier and more uniform binding of antibody on the PS surface. But for the silica surface of optical microfibers, the fabrication process makes the surface smooth. It might be hard to produce abundant oxidation groups via the oxidation by a

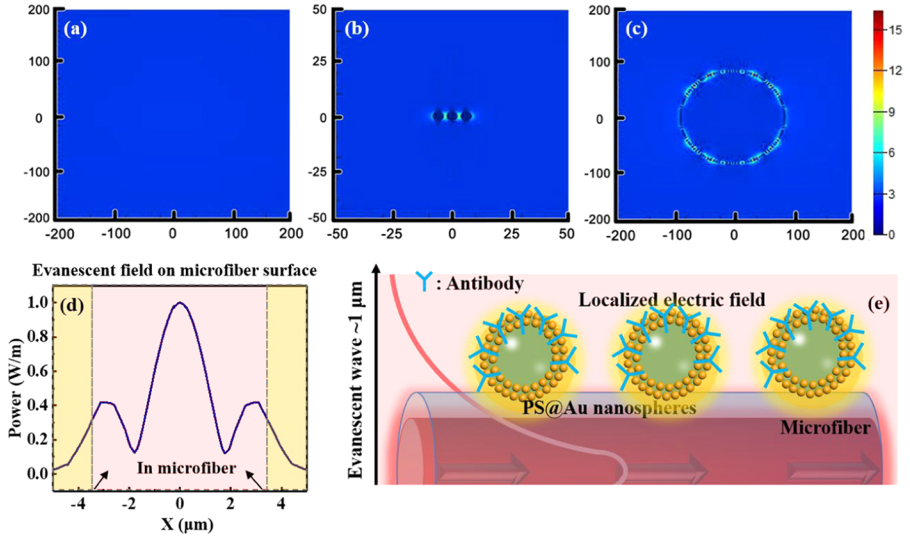

Figure 5. Near-field intensity mapping of various sensor surfaces: (a) without an interface, (b) microfiber surface functionalized by gold nanoparticles, and (c) individual PS@Au nanosphere. (d) Analyzed lateral electric field amplitude distribution of transducer's HE_{12} mode. (e) Schematic diagram of the evanescent field enhanced by the local electric field of the PS@Au nanosphere interface.

DOI: 10.1021/acsami.9b16702
ACS Appl. Mater. Interfaces 2020, 12, 1799–1805

piranha solution. Polymer surfaces are generally considered to be more easily modified than inorganic surfaces. Some works used polymer membranes to enhance the surface modifiability of silica optical fibers.[35−37]) This made the number of recognition molecular layers on the sensor surface larger, and the antibodies on the surface more stable.

On the other hand, the evanescent field intensity is also a determining factor in sensor sensitivity because the microfiber interacts with the surface matters through its evanescent field.[20] Electromagnetic enhancement is an effective way to improve the evanescent field.[23] In Figure 5a−c, the near-field intensity mappings of the various fiber surfaces at a wavelength of 1550 nm were performed by a finite-difference time-domain (FDTD) method to investigate the interfacial electromagnetic enhancement effect. From an individual gold nanoparticle (Figure S5) to gold nanoparticles, to the PS@Au nanosphere, the electric field intensity increased from approximately 4.23, to 9.02, to 16.41. (The electric field intensity on the silica microfiber surface without an interface was 1.69.) Accordingly, the localized electric field of the microfiber with an interface at 1550 nm was about ten times higher than that of the unfunctional silica surface. Figure 5d shows the calculated traverse electric field amplitude distribution of the HE_{12} mode. It shows that the penetration depth[23] was about 1 μm. Here, with a thickness of 200 nm (the diameter of the nanosphere), the monolayer nanosphere interface immobilized on the fiber surface with the localized electric field within the transducer's evanescent field and contributed to the evanescent field enhancement of the as-prepared sensor[38,39] (Figure 5e). The response of the sensor to biomolecular binding ($\Delta\lambda$) is proportional to its surface energy ($|E(x,y)|^2$, $E(x,y)$ is the surface electric field of the sensor).[40,41] That is, the sensitivity is proportional to the surface energy of the microfiber. Thus, the slight enhancement of the surface evanescent field could greatly improve the LOD.

Above all, the nanosphere interface enhanced the sensor sensitivity by increasing the interfacial assembly surface area and enhancing the electromagnetic field. Therefore, the bulk RI sensitivity of the sensor was not enhanced obviously (Figure 3e), while the surface RI sensitivity increased significantly. This microfiber is suitable for sensors monitored by the binding reaction on its surface. It can fully achieve the measurement of ultralow CEACAM5 concentrations in early-stage detection.

In Figure 6a, to evaluate the selectivity of the sensor in the actual clinical measurement, its response to CEACAM5 at a low concentration (10^{-14} M) and interfering molecules that might exist in real samples at high concentrations (glucose and sodium ions at a concentration of 10^{-6} M and IgG and ErbB2 at a concentration of 10^{-9} M) was studied. The results demonstrate that compared with the significant optical response in the CEACAM5 solution (about 3 nm), no obvious wavelength shift was recorded when the sensor was placed in the interfering molecule solutions.

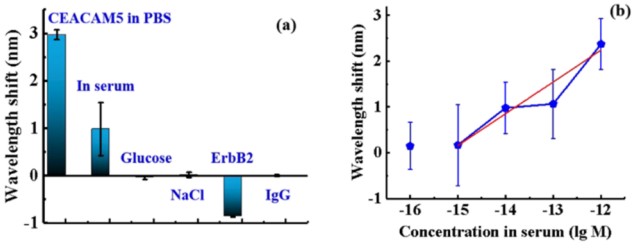

Figure 6. (a) Optical responses of the sensor versus CEACAM5 at a concentration of 10^{-14} M in PBS solution, CEACAM5 at a concentration of 10^{-14} M in 10% serum, and other interfering molecules at high concentrations in PBS solution (glucose and NaCl: 10^{-6} M; ErbB2: 10^{-9} M; IgG: 10^{-9} M). (b) Optical response of the as-prepared sensor in detecting the CEACAM5 in 10% serum at different concentrations.

Furthermore, the sensor's detection ability of CEACAM5 in 10% serum was investigated, as shown in Figure 6b. The wavelength stability of the as-prepared sensor in 10% serum solution is shown in Figure S6. With an increase in the CEACAM5 concentration from 10^{-15} to 10^{-12} M, the biosensor recorded regular redshifts in the transmission spectrum with sensitivity and LOD were 0.69 nm/lg M and 5.27×10^{-16} M, respectively. Since the tissues in serum at high concentrations could induce some energy loss, the LOD in serum is a little higher than that in the pure CEACAM5 solution.[38] However, the response is still high enough for early-stage detection. Table 1 shows a comparison of LOD of the reported CEACAM5 sensors and this work. It reveals that the LOD of the as-prepared sensor is much lower than that of the reported work.[2,8,9] This sensor is suitable as a POCT device for CEACAM5 detection in the early stage.

Table 1. Comparison of LOD of the Reported CEACAM5 Sensors and This Work

technique	LOD	references
silicon nanowires on a chip	10^{-10} M (18 ng/mL) in pure solution	8
immunohistochemistry	in tissues	2
DNA microelectrochemical biosensor	in cells	9
optical microfiber biosensor with interface	3.54×10^{-17} M in pure solution, 5.27×10^{-16} M in serum	this work

CONCLUSIONS

In this work, an ultrasensitive optical microfiber sensor functionalized with a PS@Au nanosphere interface for CEACAM5 detection at ultralow concentration has been demonstrated. With the sensitization effect of the PS@Au nanosphere interface, the LOD reached 3.54×10^{-17} M in pure solution and 5.27×10^{-16} M in serum, which is about 6 orders of magnitude lower than that of recent methods. These properties of the sensor enable early-stage detection of CEACAM5 at ultralow concentrations present in the serum as a POCT device. As the interfacial synergistic sensitization strategy is suitable for biosensors based on the surface RI sensitivity, this work provides new opportunities for the detection of biomarkers in the early stages of cancers.

EXPERIMENTAL SECTION

Materials. PBS solution (pH 7.4), CEACAM5 molecules, CEACAM5 antibody, immunoglobulin G (IgG), epidermal growth factor receptor (ErbB2), and fetal bovine serum (E600001-0500) were obtained from Sangon Inc. (Shanghai, China). Monodispersed PS nanospheres with diameters of 170 nm and monodispersed gold nanoparticles with carboxyl groups (diameter: 5 nm; No. 9-3-0005) were synthesized by BaseLine Co. (Tianjin, China). The other chemicals were obtained from Sigma-Aldrich (Shanghai) trading co. LTD. (China).

DOI: 10.1021/acsami.9b16702
ACS Appl. Mater. Interfaces 2020, 12, 1799−1805

The CEACAM5 solutions for detection were diluted with a PBS solution. IgG and ErbB2 solutions were diluted to 10^{-9} M. NaCl and glucose solutions were diluted to 10^{-6} M.

PS@Au Nanospheres. The PS@Au nanospheres used here contained a PS core (170 nm) and gold nanosatellites (5 nm), which were prepared as follows: 0.14 g of PS nanospheres was dispersed in a 3-aminopropyl-triethoxysilane (APTES) solution with stirring for 1 h. After that, the products were thoroughly washed with ethanol and dispersed in deionized water for gold nanoparticle coating. Then, 0.006 g of *N*-3-dimethylaminopropyl-*N*′-ethylcarbodiimide hydrochloride (EDC), 0.006 g of *N*-hydroxysuccinimide (NHS), and 4 mL of gold nanoparticles (concentration: 0.0478 g/L; the coverage of carboxyl groups: 28.45 μmol/g; size of Au NPs: 5 nm) were added to the PS nanosphere dispersion, and the pH value was adjusted by hydrochloric acid to 4.5, stirring at 25 °C for 20 h. The products were washed with 40 mL of ethanol and distilled water three times, respectively, centrifuged three times, and dried to obtain the PS@Au nanospheres.

PS@Au Nanosphere−Antibody. A 1 wt % solution of glutaraldehyde solution was added into the PS@Au nanosphere dispersion and stirred for 1 h. After washing the unreacted glutaraldehyde, 4 mL of CEACAM5 antibody (10 nM) was added into the PS@Au nanosphere dispersion and stirred for 5 h at 25 °C. The antibodies were immobilized on the PS surface through glutaraldehyde. The products were washed with 20 mL of distilled water three times and centrifuged.

Characterization. The morphology of PS@Au nanospheres was investigated by TEM (JEOL, JEM-2100F) with an EDS and STEM system. The UV−vis spectra were investigated by a UV−vis spectrophotometer (Shimadzu, UV-2550). The sensor surfaces were studied by field emission SEM (ZEISS, ULTRA 55).

Optical Microfiber. Figure 1 demonstrates the detection mechanism of the as-prepared biosensor. The optical microfiber was tapered through a flame-brushing method as previously described.[31] A microfiber transducer with a waist length of 4 mm and a diameter of 7.5 μm was fabricated.

This microfiber transducer was a Mach−Zehnder interferometer.[30] The HE_{11} mode and the HE_{12} mode were allowed good separation to produce the π phase shift. The uniform waist acted as an interferometer and the transmission spectrum red-shifted with increasing surface RI.

The input wavelength from the light source here was 1250−1650 nm. The power from the broadband light source was 4.28 mW and was stable in the experiment.

Immobilization of the PS@Au Nanosphere−Antibody Interface. The silica microfiber was cleaned in a piranha solution[23] to generate reactive hydroxyl groups, followed by a thorough wash and immersion in the PS@Au−antibody dispersion for 30 min. After that, the microfiber was washed. The as-prepared sensor was ready for CEACAM5 detection.

After the detection of a series of solutions with different concentrations (from 0 to 10^{-10} M), the PS@Au nanospheres and antibodies were washed off by a piranha solution. Then, the same method was used to refunctionalize the nanospheres and antibodies on the optical microfiber surface. The consistency of the properties of the interface was guaranteed by controlling the consistency of the modification conditions.

■ ASSOCIATED CONTENT

Supporting Information

The Supporting Information is available free of charge at https://pubs.acs.org/doi/10.1021/acsami.9b16702.

Wavelength stability of the as-prepared sensor in PBS solution and in serum solution, wavelength shifts of control microfiber sensor with different nanointerfaces, optical responses of the one of the control sensors without antibodies, SEM images of microfiber surface after detection, and near-field intensity mapping of the microfiber surface functionalized by individual gold nanoparticle (PDF)

■ AUTHOR INFORMATION

Corresponding Author

*E-mail: thuangyy6@jnu.edu.cn.

ORCID

Yunyun Huang: 0000-0001-7528-1001

Bai-Ou Guan: 0000-0002-3790-2986

Author Contributions

The manuscript was written through the contributions of all authors. All authors have given approval to the final version of the manuscript.

Funding

We are grateful to the National Natural Science Foundation of China (Nos. 51773084, U1701268), the Guangdong Natural Science Foundation (No. 2019A1515011278), and the Special Funds for the Cultivation of Guangdong College Students' Scientific and Technological Innovation ("Climbing Program" Special Funds, No. pdjh2019a0054).

Notes

The authors declare no competing financial interest.

■ REFERENCES

(1) Aebersold, R.; Anderson, L.; Caprioli, R.; Druker, B.; Hartwell, L.; Smith, R. Perspective: A Program to Improve Protein Biomarker Discovery for Cancer. *J. Proteome Res.* **2005**, *4*, 1104−1109.

(2) Zhou, J.; Fan, X.; Chen, N.; Zhou, F.; Dong, J.; Nie, Y.; Fan, D. J. Identification of CEACAM5 as a Biomarker for Prewarning and Prognosis in Gastric Cancer. *J. Histochem. Cytochem.* **2015**, *63*, 922−930.

(3) Shively, J. E.; Beatty, J. D. Cea-Related Antigens: Molecular Biology and Clinical Significance. *Crit. Rev. Oncol. Hematol.* **1985**, *2*, 355−399.

(4) Hammarström, S. The Carcinoembryonic Antigen (CEA) Family: Structures, Suggested Functions and Expression in Normal and Malignant Tissues. *Semin. Cancer Biol.* **1999**, *9*, 67−81.

(5) Blumenthal, R. D.; Hansen, H. J.; Goldenberg, D. M. Inhibition of Adhesion, Invasion, and Metastasis by Antibodies Targeting CEACAM6 (NCA-90) and CEACAM5 (Carcinoembryonic Antigen). *Cancer Res.* **2005**, *65*, 8809−8817.

(6) Vardakis, N.; Messaritakis, I.; Papadaki, C.; Agoglossakis, G.; Sfakianaki, M.; Saridaki, Z.; Apostolaki, S.; Koutroubakis, I.; Perraki, M.; Hatzidaki, D.; Mavroudis, D.; Georgoulias, V.; Souglakos, J. Prognostic Significance of the Detection of Peripheral Blood CEACAM5mRNA-Positive Cells by Real-Time Polymerase Chain Reaction in Operable Colorectal Cancer. *J. Clin. Cancer Res.* **2011**, *17*, 165−173.

(7) Minami, S.; Furui, J.; Kanematsu, T. Role of Carcinoembryonic Antigen in the Progression of Colon Cancer Cells That Express Carbohydrate Antigen. *Cancer Res.* **2001**, *61*, 2732−2735.

(8) Su, D. S.; Chen, P.; Chiu, H.; Han, C.; Yen, T.; Chen, H. Disease Antigens Detection by Silicon Nanowires with the Efficiency Optimization of Their Antibodies on a Chip. *Biosens. Bioelectron.* **2019**, *141*, No. 111209.

(9) Añorga, L.; Rebollo, A.; Herrán, J.; Arana, S.; Bandrés, E.; García-Foncillas, J. Development of a DNA Microelectrochemical Biosensor for CEACAM5 Detection. *IEEE Sens. J.* **2010**, *10*, 1368−1374.

(10) Gubala, V.; Harris, L. F.; Ricco, A. J.; Tan, M. X.; Williams, D. E. Point of Care Diagnostics: Status and Future. *Anal. Chem.* **2012**, *84*, 487−515.

(11) Luppa, P. B.; Müller, C.; Schlichtiger, A.; Schlebusch, H. Point-of-Care Testing (POCT): Current Techniques and Future Perspectives. *Trends Anal. Chem.* **2011**, *30*, 887−898.

DOI: 10.1021/acsami.9b16702
ACS Appl. Mater. Interfaces 2020, 12, 1799−1805

(12) Wang, P.; Bo, L.; Semenova, Y.; Farrell, G.; Brambilla, G. Optical Microfibre Based Photonic Components and Their Applications in Label-Free Biosensing. *Biosensors* **2015**, *5*, 471−499.
(13) Song, B.; Zhang, H.; Liu, B.; Lin, W.; Wu, J. Label-Free in-situ Real-Time DNA Hybridization Kinetics Detection Employing Microfiber-Assisted Mach-Zehnder Interferometer. *Biosens. Bioelectron.* **2016**, *81*, 151−158.
(14) Chiavaioli, F.; Baldini, F.; Tombelli, S.; Trono, C.; Giannetti, A. Biosensing with Optical Fiber Gratings. *Nanophotonics* **2017**, *6*, 663−679.
(15) Liu, N.; Shi, L.; Zhu, S.; Xu, X.; Yuan, S.; Zhang, X. Whispering Gallery Modes in a Single Silica Microparticle Attached to an Optical Microfiber and Their Application for Highly Sensitive Displacement Sensing. *Opt. Express* **2018**, *26*, 195−203.
(16) Li, J.; Sun, L.; Gao, S.; Quan, Z.; Chang, Y.; Ran, Y.; Jin, L.; Guan, B. Ultrasensitive Refractive-Index Sensors based on Rectangular Silica Microfibers. *Opt. Lett.* **2011**, *36*, 3593−3595.
(17) Fan, X.; White, I. M.; Shopova, S. I.; Zhu, H.; Suter, J. D.; Sun, Y. Sensitive Optical Biosensors for Unlabeled Targets: A Review. *Anal. Chim. Acta* **2008**, *620*, 8−26.
(18) Tazawa, H.; Kanie, T.; Katayama, M. Fiber-Optic Coupler Based Refractive Index Sensor and Its Application to Biosensing. *Appl. Phys. Lett.* **2007**, *91*, No. 113901.
(19) Wei, T.; Han, Y.; Tsai, H.-L.; Xiao, H. Miniaturized Fiber Inline Fabry-Perot Interferometer Fabricated with a Femtosecond Laser. *Opt. Lett.* **2008**, *33*, 536−538.
(20) Guan, B.; Huang, Y. Interface Sensitized Optical Microfiber Biosensors. *J. Lightwave Technol.* **2019**, *37*, 2616−2622.
(21) Huang, Y.; Ding, M.; Guo, T.; Zhang, N.; Tian, Z.; Sun, L.; Guan, B. Ultrasensitive and Label-Free Detection of γ-Aminobutyric Acid Using Fiber-Optic Interferometric Sensors Functionalized with Size-Selective Molecular Sieve Arrays. *Sens. Actuators, B* **2017**, *244*, 934−940.
(22) Sridevi, S.; Vasu, K. S.; Asokan, S.; Sood, A. K. Sensitive Detection of C-Reactive Protein Using Optical Fiber Bragg Gratings. *Biosens. Bioelectron.* **2015**, *65*, 251−256.
(23) Li, H.; Huang, Y.; Chen, C.; Xiao, A.; Hou, G.; Huang, Y.; Feng, X.; Guan, B. Real-Time Cellular Cytochrome C Monitoring through an Optical Microfiber: Enabled by a Silver-Decorated Graphene Nanointerface. *Adv. Sci.* **2018**, *5*, No. 1701074.
(24) Hu, H.; Dai, A.; Sun, J.; Li, X.; Gao, F.; Wu, L.; Fang, Y.; Yang, H.; An, L.; Wu, H.; Yang, S. Aptamer-Conjugated Mn_3O_4@SiO_2 Core-Shell Nanoprobes for Targeted Magnetic Resonance Imaging. *Nanoscale* **2013**, *5*, 10447−10454.
(25) Caruso, F.; Spasova, M.; Salgueiriño-Maceira, V.; Liz-Marzán, L. M. Multilayer Assemblies of Silica-Encapsulated Gold Nanoparticles on Decomposable Colloid Templates. *Adv. Mater.* **2001**, *13*, 1090−1094.
(26) Haiss, W.; Thanh, N. T. K.; Aveyard, J.; Ferning, D. G. Stability and Catalytic Activity of PEG-b-PS-Capped Gold Nanoparticles: A Matter of PS Chain Length. *Anal. Chem.* **2007**, *79*, 4215−1221.
(27) Mansur, H. S.; Sadahira, C. M.; Souza, A. N.; Mansur, A. A. P. FTIR Spectroscopy Characterization of Poly (vinyl alcohol) Hydrogel with Different Hydrolysis Degree and Chemically Crosslinked with Glutaraldehyde. *Mater. Sci. Eng. C* **2008**, *28*, 539−548.
(28) Shen, B.; Zhai, W.; Chen, C.; Lu, D.; Wang, J.; Zheng, W. Melt Blending in situ Enhances the Interaction between Polystyrene and Graphene through π-π Stacking. *ACS Appl. Mater. Interfaces* **2011**, *3*, 3103−3109.
(29) Pasternack, R. M.; Amy, S. R.; Chabal, Y. J. Attachment of 3-(Aminopropyl) triethoxysilane on silicon Oxide Surfaces: Dependence on Solution Temperature. *Langmuir* **2008**, *24*, 12963−12971.
(30) Lou, J.; Wang, Y.; Tong, L. Microfiber Optical Sensors: A Review. *Sensors* **2014**, *14*, 5823−5844.
(31) Tan, Y.; Sun, L.; Jin, L.; Li, J.; Guan, B. Microfiber Mach-Zehnder Interferometer based on Long Period Grating for Sensing Applications. *Opt. Express* **2013**, *21*, 154−156.
(32) Leung, A.; Shankar, P. M.; Mutharasan, R. A Review of Fiber-optic Biosensors. *Sens. Actuators, B* **2007**, *125*, 688−703.
(33) Liu, M.; Liu, R.; Chen, W. Graphene Wrapped Cu_2O Nanocubes: Non-enzymatic Electrochemical Sensors for the Detection of Glucose and Hydrogen Peroxide with Enhanced Stability. *Biosens. Bioelectron.* **2013**, *45*, 206−212.
(34) Javkhlantugs, N.; Bayar, H.; Ganzorig, C.; Ueda, K. Computational Study on the Interactions and Orientation of Monoclonal Human Immunoglobulin G on a Polystyrene Surface. *Int. J. Nanomed.* **2013**, *8*, 2487−2496.
(35) Marks, R. S.; Novoa, A.; Thomassey, D.; Cosnier, S. An Innovative Strategy for Immobilization of Receptor Proteins on to an Optical Fiber by Use of Poly(pyrrole-biotin). *Anal. Bioanal. Chem.* **2002**, *374*, 1056−1063.
(36) Wang, X.; Wolfbeis, O. Fiber-Optic Chemical Sensors and Biosensors. *Anal. Chem.* **2016**, *88*, 203−227.
(37) Uzun, L.; Turner, A. P. F. Molecularly-Imprinted Polymer Sensors: Realizing Their Potential. *Biosens. Bioelectron.* **2016**, *76*, 131−144.
(38) Lepinay, S.; Staff, A.; Ianoul, A.; Albert, J. Improved Detection Limits of Protein Optical Fiber Biosensors Coated with Gold Nanoparticles. *Biosens. Bioelectron.* **2014**, *52*, 337−344.
(39) Renoirt, J.; Debliquy, M.; Albert, J.; Ianoul, A.; Caucheteur, C. Surface Plasmon Resonances in Oriented Silver Nanowire Coatings on Optical Fibers. *J. Phys. Chem. C* **2014**, *118*, 11035−11042.
(40) Liang, L.; Jin, L.; Ran, Y.; Sun, L.; Guan, B. Interferometric Detection of MicroRNAs using a Capillary Optofluidic Sensor. *Sens. Actuators, B* **2017**, *242*, 999−1006.
(41) Kim, E.; Baaske, M. D.; Vollmer, F. Towards Next-Generation Label-Free Biosensors: Recent Advances in Whispering Gallery Mode Sensors. *Lab Chip* **2017**, *17*, 1190−1205.

DOI: 10.1021/acsami.9b16702
ACS Appl. Mater. Interfaces 2020, 12, 1799−1805